machines

MDPI

Article

The Tightening and Untightening Modeling and Simulation of Bolted Joints

Rashique Iftekhar Rousseau * and Abdel-Hakim Bouzid

Department of Mechanical Engineering, École de Technologie Supérieure, Montreal, QC H3C 1K3, Canada; hakim.bouzid@etsmtl.ca

* Correspondence: rashique-iftekhar.rousseau.1@ens.etsmtl.ca

Abstract: Although bolted joints may appear simple and are easy to manipulate, they are challenging to model and analyze due to their complex structural patterns and statically indeterminate nature. Ensuring the structural integrity of these joints requires maintaining proper bolt preload and clamping force, which is crucial for preventing failures such as overload, excessive bearing stress, fatigue, and stripping caused by seizing or galling. Achieving the necessary clamping force involves carefully controlling the input tightening torque, which is divided into the pitch torque and the friction torques at the bolt or nut bearing surfaces and in the engaged threads. The resulting clamping force is critical for generating the required force within the bolt. However, the achieved bolt force depends on several factors, such as friction at the joint's contact surfaces, grip length, and the relative rotation between the bolt and nut during tightening. Friction at the contact surfaces, particularly beneath the bolt head or nut and between the threads, consumes a significant portion of the applied tightening torque—approximately 90%. This paper explores the three existing bolt internal pitch, bearing, and thread friction torques that are generated by the external applied torque in a bolted joint, as well as their contributions and variations throughout a loading cycle composed of three phases: tightening, settling, and untightening. An analytical model is developed to determine these torque components, and its results are compared with those obtained from finite element (FE) modeling and experimental testing from previous studies. Finally, this study examines the torque–tension relationship during bolt tightening, offering insights into the required accuracy of bolt and clamped member stiffness. The bolt samples used in this study include M12 × 1.75 and M36 × 4 hex bolts.

Keywords: threaded fastener; joint tightening and untightening; stiffness; friction torque; pitch torque

Citation: Rousseau, R.I.; Bouzid, A.-H. The Tightening and Untightening Modeling and Simulation of Bolted Joints. *Machines* **2024**, *12*, 654. https://doi.org/10.3390/machines12090654

Academic Editor: António Bastos Pereira

Received: 23 July 2024
Revised: 5 September 2024
Accepted: 11 September 2024
Published: 19 September 2024

1. Introduction

Among the non-permanent clamping methods, bolted joints are the most popular, as they provide easier features for their assembling and disassembling. Having sufficient clamping force in a bolted joint is very important as it ensures structural integrity and reliability of the clamped products. In the bolted joints, the bolt force generated due to tightening depends on the torque applied on the bolt, which is critical to estimate as it is dependent on certain conditions, such as the material specifications, contact surface conditions, and the type of threads. Insufficient torque results in a joint with inadequate clamping force, whereas an excessive amount of torque can be the reason for joint failure, and therefore possible damage to the components can take place. It is thus important to determine the proper installation torque for a bolted joint to ensure sufficient clamping force to avoid joint separation as well as overstretching of the bolt.

Several factors must be considered when determining the input tightening torque, as the clamping force can vary with the identical input torque. These include joint geometry, material strength, inclusion of washers, contact surface conditions, and types of loadings [1]. Frictions at different contact surfaces are highly important to count in, as small variations

in friction torques bring significant change in the torque as well as in joint tension. The first torque–tension relationship was presented by Motosh [2] for threaded joints as follows:

$$T_e = F_b\left(\frac{p}{2\pi} + \frac{\mu_t r_t}{\cos\beta} + \mu_b r_b\right) \quad (1)$$

where T_e = external input torque, F_b = bolt load, p = thread pitch, μ_t = thread friction coefficient, μ_b = bolt head bearing friction coefficient, β = thread profile angle (half), r_b = effective bearing friction radius, and r_t = effective thread friction radius. The three components on the right-hand side of Equation (1) are three different torque components known as pitch torque T_p, thread friction torque T_t, and bolt head bearing friction torque T_b, respectively. The tension or preload in the bolted joint is developed by the pitch torque component T_p, which provides the clamping force in the joint by stretching the bolt. On the contrary, the other two torque components, T_b and T_t, are used to overcome the friction at contact surfaces: the former being in between the bolt head or nut and the corresponding clamped member surface in contact, and the latter between the engaged threads of the bolt and nut. Though this equation is a strong basis of the torque-tightening method, lack of accuracy of the tightening torque resulted from not considering the thread helix angle, effective radii of bearing and thread contacts, and contact pressure distribution. Usually, almost 90% of the input tightening torque is consumed by the two frictional torque components [3]. Also, the clamping force of a bolted joint highly depends on the friction coefficients at different contact surfaces, as small changes in the roughness percentages of the joint parts can significantly change the predicted amount of clamping force and thus affect the joint stability [3,4]. Although the values of friction coefficients can be known based on the material being used, in real practice these values change as the contact surfaces and the techniques highly depend on the contact surface geometries, loading, and environmental factors [5]. Therefore, it is highly important to properly determine these friction coefficients for the accurate measurement of friction torques that in turn provide the required clamping force of the joint and ensure its integrity. Inaccurate measurement of T_b can lead to joint leakage, separation, loosening, and fatigue failure, whereas T_t can cause material failure because of overstress.

Several studies have been conducted on developing the correlation between the input torque and the clamping force of joints. Nassar and Yang [6] performed a study on developing an analytical relationship between tightening torque and clamping force for joint applications where a difference was shown between theoretical and experimental results of clamping force by a torque-angle control technique. In another study, Nassar and Zaki [7] tested the impact of coating thickness and showed a noticeable effect of the bearing and thread friction coefficients, highlighting the sensitive impact of frictional changes on the torque–clamping force relationship. The torque equation of Motosh discussed earlier was improved by Nassar and his colleagues [8,9], where they presented analytical models of effective radii of bearing and thread frictions to calculate bearing and thread friction torques, respectively. The former highlighted the significance of correctly determining the bearing friction coefficient considering four different contact pressure distribution scenarios on a bearing surface, whereas the latter focused on analytically improving the thread friction torque component considering five complex pressure distribution scenarios between the mating thread surfaces in contact. Izumi et al. [10] highlighted a deviation coming up from the comparison of the preload–tightening torque relationship with that from classical theory due to the underestimation of non-uniform contact pressure at a bolt bearing surface. Contrary to conventional theory, they figured out the starting point of joint loosening as due to the occurrence of complete thread slip before bolthead slip occurs under shear loading, which is a key point to consider in the joint design for preventing early loosening. Huang and Julo [11] restructured the torque–tension relationship considering all the forces and moments that act in the bolted joints instead of only relying on axial force as carried out earlier in the classic method by Motosh. They used FE modeling to validate their results. Fukuoka [12] showed the importance of the tightening method with

a hydraulic tensioner over the torque method because the former does not get influenced by the helical friction coefficient of mating threads and circumferential friction coefficients on the bolt or nut bearing surfaces, thus giving less error. He evaluated the effective tensile coefficient, the ratio of required clamping force to the initial tension, which has the primary influence of grip length with minimal impact of bolt nominal diameter.

Jiang et al. [13] experimentally found that the friction coefficients in a bolted joint can be affected by repeated tightening. The bearing friction coefficient does not change much after repeated tightening, but the thread friction coefficient tends to increase after a certain number of tightening and untightening. Liu et al. [14] also noticed while investigating the behavior of friction coefficients under repeated tightening that the friction coefficients become higher by repeated tightening without lubrication. However, friction coefficients tend to stabilize or decrease with lubrication after repeated tightening. The impact of different types of lubricants was experimentally investigated by Zou et al. [15] in altering the torque–tension relationship and the friction coefficients of a bolted joint. Among the three, the solid-film lubricant types gave lower friction coefficient values compared to the greases and oils, thus providing a higher clamping force with the same input torque. Grabon et al. [16] experimentally studied the impact of tribological factors on the contact surfaces of bolted joints to understand how the actual contact area between surfaces changes during tightening, which is complex to predict. They found higher values for bearing friction coefficient compared to that for engaged thread when tightening and observed a parabolic increase of total tightening torque instead of having linearity as per standard expectation. Nonetheless, a quantitative benchmark to evaluate the tightening performance is lacking, thus making the approach less feasible for industrial applications. Fernando et al. [17] formulated the relationship between bolt tension and torque, considering the three-dimensional thread helical geometry and the nut dilation effect, improving upon Nassar's model [5]. Jiang et al. [18] developed a model based on Motosh's theory [2] to investigate the distribution of input torque using the energy method, where the effects of parameters such as effective bearing contact radius, thread contact radius, and spiral angle were analyzed. Zhang et al. [19] introduced an innovative method to enhance the torque–tension relationship of threaded fasteners by incorporating a differential geometric representation of the thread surface and accounting for pressure distribution on contact surfaces.

However, there is still a lack of studies to answer the concerns regarding how various torque components are distributed in the joint contact surfaces and how they act while the joint undergoes tightening and untightening cycles and remains at rest in between. This paper proposed a detailed finite element-based method to evaluate individual contributions of the three torque components: bearing friction torque between the bolt head or nut and the corresponding clamped member in contact, thread friction torque between engaged threads, and pitch torque in a bolted joint, and their variations during tightening, untightening, and states at rest condition between both cycles. A three-dimensional (3D) M12 $\times$ 1.75 hex bolt is modeled, including threads to imitate the joint-tightening and untightening phenomena through bolt and nut relative rotation for analyzing the relationship among the external input torque, resulting bolt force, and rotation between the bolt and the nut. The bolted joint undergoes tightening and untightening cycles with different values of friction coefficients for bearing and thread contacts to observe the correlation between bolt force and input torque.

2. Analytical Model

It is important to consider the equilibrium condition to properly analyze the assembly of a tightened bolted joint made up of a bolt, a nut, and two clamped members held together by friction. The input torque applied to tighten the joint must be of an amount enough to overcome the torques resulting from the friction forces under the bolt head T_b and in between the engaged threads T_t to resist rotation, as shown in Figure 1. Therefore, external input torque $T_e \geq T_b + T_t$ [20].

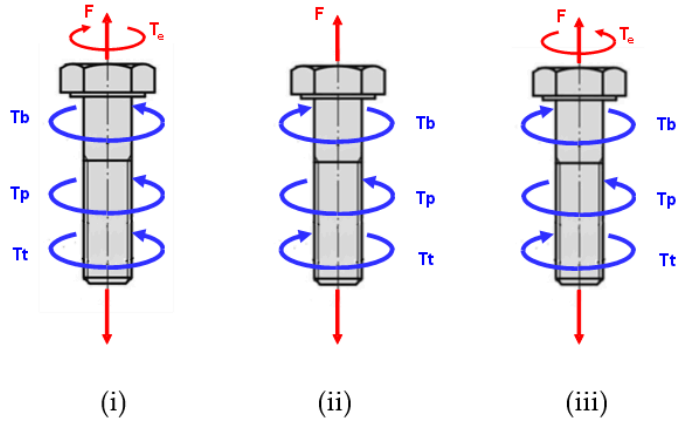

Figure 1. Moment equilibrium: (**i**) tightening, (**ii**) at rest after tightening, and (**iii**) untightening.

The pitch torque T_p resulting from the contact pressure on engaged threads acts in the loosening direction. Thus, the following equilibrium conditions occur during the tightening and untightening of the joint:

$$\begin{gathered} T_e \geq T_b + T_t + T_p \text{ (tightening)} \\ T_b + T_t - T_p = 0 \text{ or, } T_p = T_b + T_t \text{ (at rest after tightening)} \\ T_e \geq T_b + T_t - T_p \text{ (untightening)} \end{gathered} \tag{2}$$

2.1. Underhead Bearing Friction Torque

While tightening the bolt, the uniform contact pressure acting under the bolt head is $p_b = F_b/A_b$, where F_b is the bolt tension force, $A_b = \pi(r_{bo}^2 - r_{bi}^2)$ is the area of the bolt underhead, and r_{bo} and r_{bi} are the maximum and minimum radii of the underhead contact surface area. The equilibrium of the elementary forces can be written as

$$\vec{dF_{Teb}} + \vec{dF_{Tbf}} = \vec{0} \tag{3}$$

where T_{eb} is the tightening torque in the contact surface area under the bolt head, $\vec{dF_{Teb}} = dF_{Teb}\vec{v}ds$ and $\vec{dF_{Tbf}} = \mu_b p_b \vec{v} ds$, as illustrated in Figure 2. μ_b is the friction coefficient of the contact surface between the bolthead and the clamped member in contact. $\vec{i}$ and $\vec{j}$ are the radial and tangential unit vectors, respectively. The bearing friction torque T_b resulting from the friction force F_{Tbf} under the bolt head opposes the tightening input torque under head T_{eb}; therefore, $T_b = T_{eb}$. The elementary bearing friction torque dT_b due to $\vec{dF_{Tbf}}$ is calculated as

$$dT_b = \left(\vec{r} \times \vec{dF_{Tbf}}\right) \cdot \vec{k} = \mu_b p_b \left(\vec{r} \times \vec{v}\right) \cdot \vec{k} ds = \mu_b p_b r^3 dr d\theta \tag{4}$$

where $ds = rdrd\theta$ for the plane contact surface. By integrating Equation (4) on the contact area, the bearing friction torque T_b can be found as follows:

$$T_b = \mu_b \iint_{\Omega_b} p_b r^3 dr d\theta \tag{5}$$

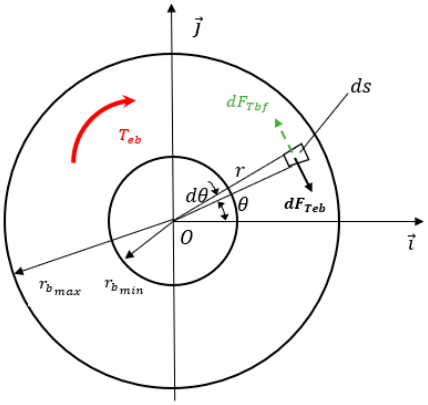

Figure 2. Free body diagram of friction on underhead bearing contact surface.

2.2. Thread Friction and Pitch Torques

Following a similar approach, the force equilibrium equation with the bolt being tightened is composed of the elementary friction force in the thread contact surface resulting from the tightening input torque T_{et} (Figure 3). In addition, pitch torque is added. Therefore,

$$\vec{dF_{Tet}} + \vec{dF_{Tp}} + \vec{dF_{tf}} = \vec{0} \tag{6}$$

where $\vec{dF_{Tp}}$ is the elementary thread pitch force. $\vec{dF_{Tp}} = \mu_t p_t \vec{v} ds$ is the elementary friction force and μ_t is the friction coefficient of the thread contact surface. $p_t = (F_b/A_t) \cdot \vec{w_1}$ is the average contact pressure where $A_t = n\pi(r_{bo}^2 - r_{bi}^2)$ is the thread contact area; r_{to} and r_{ti} are the maximum and minimum radii of the thread contact area, respectively. n is the number of engaged threads. $\vec{w_1}$ is the unit vector normal to the thread contact surface, which is defined by the cross product of radial and tangential vectors $\vec{u_r}$ and $\vec{v_t}$ that are parallel to the thread contact surface. Therefore,

$$w_1 = \frac{\vec{u_r} \times \vec{v_t}}{\left|\vec{u_r}\right|\left|\vec{v_t}\right|} = \cos\alpha \cos\beta \begin{bmatrix} \tan\alpha \\ \tan\beta \\ 1 \end{bmatrix} \tag{7}$$

where α and β are the half of the thread profile angle and the thread helix angle, respectively. $\vec{u_r}$ and $\vec{v_t}$ can be found from the local coordinate system $(\vec{u}\,\vec{v}\,\vec{w})$, as shown in Figure 2:

$$\vec{u_r} = \begin{bmatrix} \cos\alpha \\ 0 \\ -\sin\alpha \end{bmatrix} \text{ and } \vec{v_t} = \begin{bmatrix} 0 \\ \cos\beta \\ -\sin\beta \end{bmatrix} \tag{8}$$

The elementary thread pitch force in the loosening direction can be written as

$$\vec{dF_{tp}} = p_t(\vec{w_1} \cdot \vec{v}) \cdot \vec{v} ds \tag{9}$$

Here, $ds = rdrd\theta/(\vec{w_1} \cdot \vec{w})$ is the elementary thread contact surface. The equilibrium equation of torques about the joint axis center O is given by

$$T_{et} = T_t + T_p \tag{10}$$

The thread pitch torque T_p can be written as follows:

$$T_P = \iint_{\Omega_t} \left(\vec{r} \times \vec{dF_{Tp}}\right) \cdot \vec{k} = \tan\beta \iint_{\Omega_t} p_t r^2 drd\theta \tag{11}$$

The thread friction torque $d\vec{F}_{Tf}$ due to the force can be given by

$$T_t = \iint_{\Omega_t} \left(\vec{r} \times d\vec{F}_{tf} \right) \cdot \vec{k} = \mu_t \cos\alpha \cos\beta \iint_{\Omega_t} p_t r^2 dr d\theta \tag{12}$$

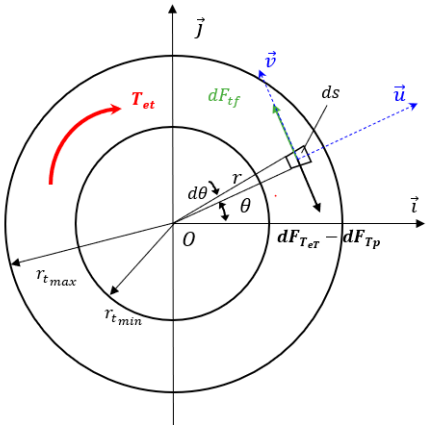

Figure 3. Free body diagram of friction on thread contact surface.

2.3. Stiffness of Joint

The total stiffness of the bolted joint, considering all its components are in series, results from the stiffness of the individual components, which can be expressed by the following equation:

$$\frac{1}{k_j} = \frac{1}{k_{sh}} + \frac{1}{k_m} + \frac{1}{k_{tc}} \tag{13}$$

where subscripts *j*, *sh*, *m*, and *tc* stand for joint, shank and head, member, and threaded connection.

2.3.1. Bolt Stiffness

The stiffness of the bolt, including its head and shank, is as follows:

$$k_{sh} = \frac{A_b E_b}{L_{eq}} = \frac{\pi d^2 E_b}{4 L_{eq}} \tag{14}$$

Here, $L_{eq} = L + 0.2\{(d^2 + H^2)/H\}$ is the equivalent bolt length with the joint grip length L and the portion resulting from the combination of bolt diameter and head thickness. A few studies came up with different recommendations to calculate L_{eq} based on a single parameter, such as adding 50% of bolt head and nut thickness each [3], 40% of head and nut diameter each [21], or 60% of head diameter and 70% of nut diameter [22]. A recent study [23] showed a noticeable impact of the combination of bolt nominal diameter and head thickness on L_{eq} and recommended using 20% of the parameter $\{(d^2 + H^2)/H\}$ to add in the calculation.

2.3.2. Stiffness of Threaded Connection

The stiffness of the threaded connection that includes the nut and part of the bolt that is threaded to it can be written as follows [24]:

$$k_{tc} = \frac{1}{\lambda(\delta_b + \delta_n)\sin\beta} \cdot \frac{\cosh\lambda M - 1}{\sinh\lambda M} \tag{15}$$

where subscripts b and n are used for bolt and nut, respectively. M is the nut height. $\lambda = \left\{(1/A_b E_b + 1/A_n E_n)/\left(1/k_{by} + 1/k_{ny}\right)\right\}^{1/2}$. $k_{by} = 1/\delta_b \sin\beta$ and $k_{ny} = 1/\delta_n \sin\beta$ are the stiffness of the unit axial length of the bolt and nut due to the unit force, respectively.

δ is the total axial elastic deformation of the thread, which is composed of thread bending deformation δ_1, thread shear deformation δ_2, thread root inclination deformation δ_3, thread root shear deformation δ_4, and radial extended deformation for the nut or radian shrinkage deformation for the bolt δ_5. Therefore, for the bolt,

$$\begin{aligned}\delta_b &= \delta_{1b} + \delta_{2b} + \delta_{3b} + \delta_{4b} + \delta_{5b} \\ &= 0.034\left(\frac{1-v_b^2}{E_b}\right) + 1.08\left(\frac{1+v_b}{E_b}\right) + 0.229\left(\frac{1-v_b^2}{E_b}\right) + 1.18\left(\frac{1-v_b^2}{E_b}\right) + 0.056(1-v_b)\frac{d_p}{E_b p}\end{aligned} \tag{16}$$

and for the nut,

$$\begin{aligned}\delta_n &= \delta_{1n} + \delta_{2n} + \delta_{3n} + \delta_{4n} + \delta_{5n} \\ &= 0.073\left(\frac{1-v_n^2}{E_n}\right) + 1.15\left(\frac{1-v_b}{E_n}\right) + 0.294\left(\frac{1-v_n^2}{E_n}\right) + 1.14\left(\frac{1-v_n^2}{E_n}\right) + 0.056\left(\frac{d_n^2+d_p^2}{d_n^2-d_p^2} + v_n\right)\frac{d_p}{E_n p}\end{aligned} \tag{17}$$

where v and E are the Poisson's ratio and Young's modulus, p is the pitch, and d_p and d_n are the pitch diameter of the bolt and the outer diameter of the nut, respectively [24].

2.3.3. Stiffness of Clamped Members

The same study [23] also proposed a more accurate method to calculate the stiffness of clamped members k_m for bolts of different sizes based on the bolt head bearing contact width instead of joint hole diameter previously used by many studies. The stiffness of the clamped members is expressed as follows:

$$k_m = \left[2.0726\left(\frac{w}{L}\right) + 0.6134\right] E_m d_h \tag{18}$$

Here, w and d_h are bearing contact width and hole diameter, respectively.

2.4. Angle of Nut Rotation

Assuming no plastic deformation, the angle of rotation of the nut with respect to the bolt to generate a force is given by

$$\theta = \frac{2F_b\pi}{pk_j} + \frac{F_b\left(\frac{p}{2\pi} + \frac{\mu_t r_t}{\cos\beta}\right)}{G_b J_b / L_{eq}} \tag{19}$$

where $G_b = E_b/2(1+v_b)$ is the shear modulus and $J_b = \pi d^4/32$ is the polar moment of area of bolt. The first term of Equation (19) refers to the nut rotation due to the axial displacement of all the joint components, whereas the second term corresponds to the nut rotation caused by the twisting of the bolt shank as a result of the applied external torque.

2.5. Nut Factor

The nut factor is an experimentally derived constant that links the external applied torque T_e to the resulting preload F_b. The equation is given by

$$T_e = F_b K d \tag{20}$$

The dimensionless nut factor K accounts for factors influencing the generation of the load, including the stiffness of the joint as a result of torsion, bending, and material deformation of all components, but mostly the effect of friction between them. However, for a specific lubricant, it must be determined experimentally, although it may not be a single number. In addition, the preload corresponding to an input torque can only be predicted within a range. Also, the nut factors evaluated in laboratory conditions often show noticeable differences from those existing in real practice; this assessment encompasses various factors including operator proficiency, tool precision, bolting techniques, as well as lubrication and thread conditions [3].

Therefore, most of the lubricant manufacturers and research laboratories do not use the nut factor but rather rely on test results based on the coefficient of friction in general. It can be calculated using the tightening external torque T_e of Equations (2) and (20) such that

$$K = \frac{T_b + T_t + T_p}{F_b d} \tag{21}$$

The pitch, bearing, and thread friction torques T_p, T_b, and T_t are given by Equations (5), (11), and (12). From Equations (1) and (20), an expression of the nut factor can be found in terms of the coefficient of friction as follows:

$$K = \frac{\frac{p}{2\pi} + \frac{\mu_t r_t}{\cos\beta} + \mu_b r_b}{d} \tag{22}$$

3. Finite Element Model

Figure 4 represents the schematic of the entire bolted joint with its various components, which consists of a M12 × 1.75 hex bolt, a nut, and two clamped members, each with an equal thickness of 10 mm in this case. The thread dimensions of the bolt and nut used in this analysis are based on the British Standard ISO Metric Screw Threads (BS 3643) [25]. ANSYS workbench [26] is used to develop the complex 3D model with hexagonal geometries of a bolt and nut, including threads (Figure 5). The mechanical properties of the bolt, nut and clamped members are listed in Table 1. All the dimensions are based on the standard, including the single-side contact interface between the mating threads to enhance the model's relevance to practicality. Since this study aims at investigating and determining accurate values of the torque components at contact surfaces to ensure proper joint-clamping force and a very small change in the friction coefficient values significantly amplifies these parameters, it is necessary to consider such 3D complex geometry into modeling even though the entire process is computationally expensive and time-consuming. To resolve this issue, a high-performance computer (HPC) is used for running the model.

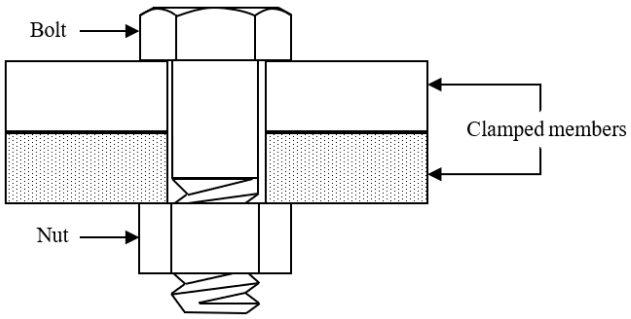

Figure 4. Schematic of a bolted joint with its components.

Table 1. Mechanical properties of bolt and nut (SA-193 B7) [27] and clamped members (SA-285 Gr C) [28].

Material Properties	Bolt and Nut (SA-193 B7)	Clamped Member (SA-285 Gr C)
Ultimate tensile strength [MPa]	860	450
Yield strength [MPa]	720	205
Young's Modulus [GPa]	206.8	206.8
Poisson's ratio	0.3	0.3

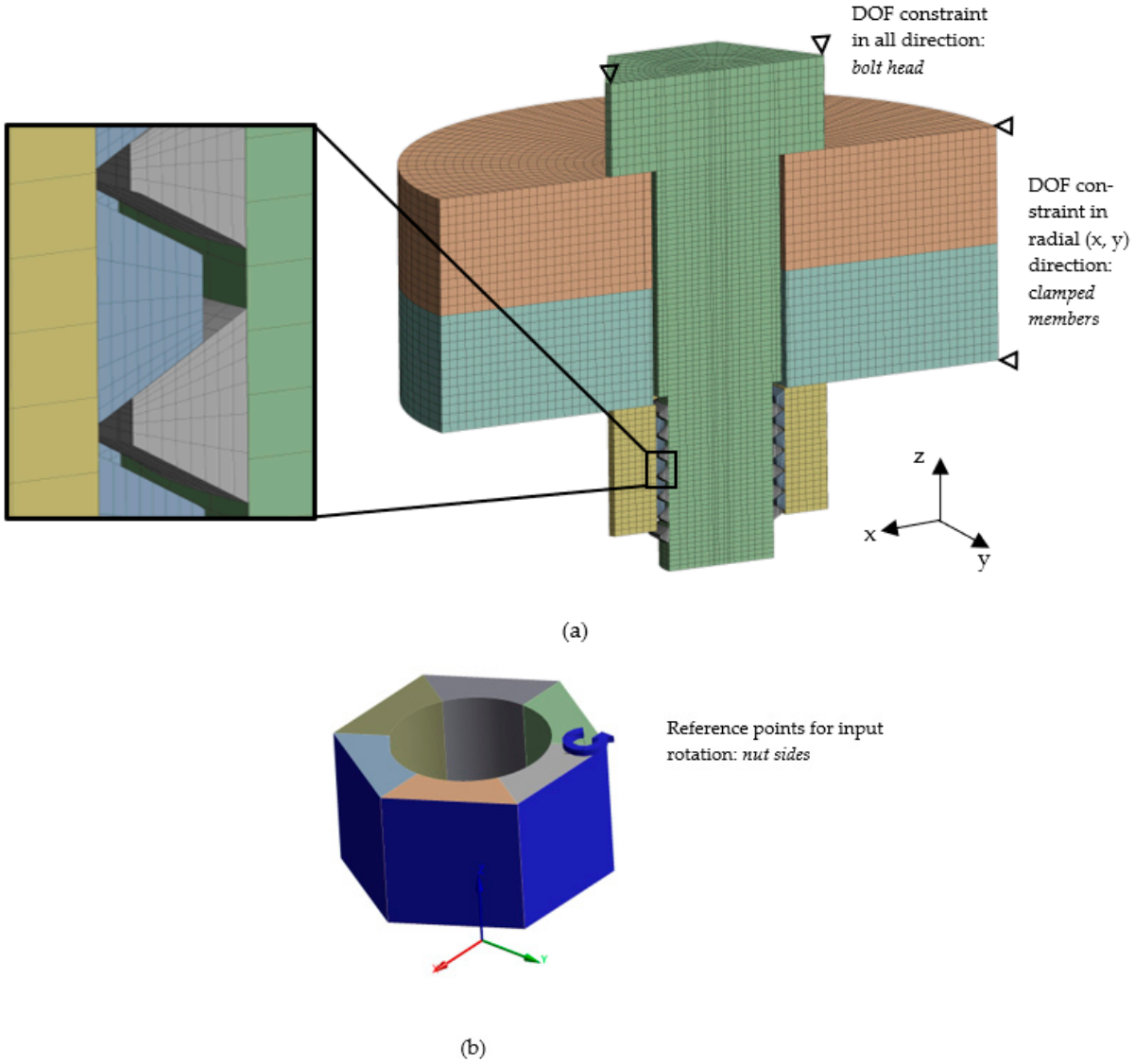

Figure 5. Three-dimensional FE model of bolted joint showing engaged thread elements: (**a**) complete model with constraints and thread mesh details; (**b**) nut rotation.

Constraints

To prevent spatial displacement of the model, singularity, and rigid body motion, horizontal displacement constraints are applied to two diametrically opposed symmetrical points of the upper and lower plates while allowing axial displacement of the bolt, as shown in Figure 5a. The preload is generated in the bolt by application of an external rotation to the nut, while the bolt is fixed in rotation and other degrees of freedom of the nut are restrained. Target and contact elements are used between the clamped members, between the bolt head and the upper clamped member, and between the nut and the lower clamped member. The bolt friction coefficient is set to 0.12, a commonly used value for metal-to-metal contact surfaces of the bolt.

The FE methodology involves tightening of the joint by applying torque T_e to induce the required amount of bolt force F_b and then untightening the joint with reverse torque to bring the clamping force down while recording the levels of the different torque components. Therefore, the joint is first tightened gradually in steps to achieve a clamping force of around 41 kN with a torque of 81 kN/mm. Since the model has a threaded bolt and nut, the preload is achieved by applying a proper amount of rotation to the nut as shown in Figure 5b. The next step is to untighten the bolt by applying a rotation to the nut in the opposite direction to

loosen the joint to 25 kN. The torque required for the untightening is lower than the tightening torque as the thread pitch torque component T_p acts in the loosening direction [18].

The model uses a structured hexahedral mesh, which offers advantages not only in reducing CPU time but also in extracting data. Especially the nut bearing and the engaged thread contact surfaces are the important contact regions where sufficient mesh refinements are performed by continuous increment of the number of elements until 1% convergence on the thread contact pressure is obtained in the engaged thread and nut and underhead bearing contact surfaces. The final model consists of 172720 elements in total.

4. Results and Discussion

Figure 6 shows the comparison between the result from the analytical model described earlier and the experimental result of Eccles [27] from the tests conducted on M12 standard hex bolts and nuts with low coefficients of friction of 0.061 and 0.07, respectively, during tightening and untightening. The analytical model curves for the tightening and untightening of the joint match well the experimental data. It is to be noted that the untightening of the joint requires a lesser amount of torque compared to that of the tightening. According to the result, the developed analytical model can replicate accurately the actual cycle of the tightening and untightening of any size bolt used with any lubricant.

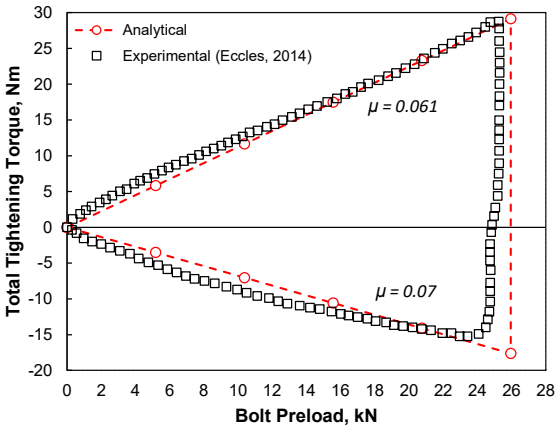

Figure 6. Comparison of analytical and experimental results [29] showing tightening and untightening stages.

A correlation between the bolt force and the required angle of rotation of the nut to achieve the bolt force is presented in Figure 7, where both the analytical and FE model results are compared with the same coefficient of friction for the bolt and threads, $\mu = \mu_b = \mu_t = 0.12$. The external torques required in both models are in close agreement with each other.

A slight nonlinearity is observed with the FE results of external torque as a function of nut rotation in the beginning because initially the contact surface of the threads under the nut and head is partial; thus, the load is not evenly distributed, making the joint less rigid. The remaining matting surfaces get in contact with further nut rotation. When the settlement of the bearing surfaces is completed, after around 3°, the curve becomes linear. As a result, a slightly higher nut rotation is observed with FEM in the beginning of the tightening as compared to the analytical results to achieve the desired amount of torque and bolt force.

Since both the analytical and FE models show reasonable agreement in reproducing the tightening and untightening processes for a particular friction coefficient so far, it is better to investigate other friction conditions, including no friction as well. Figure 8 gives an overall picture of both the tightening and untightening torques for different friction coefficients for the M12 hex bolt. A comparison among the results of FE, the analytical model, and the Motosh model (Equation (1)) shows perfect agreement for all friction conditions. Since the Motosh equation is a simplified version for torque evaluation and is

limited to only tightening loads and single bolted joints concentric with the bolt axis [3], the current model can be considered an improvement without such limitations.

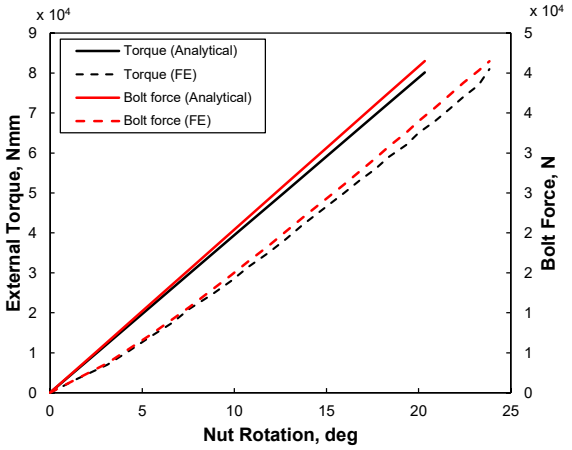

Figure 7. Torque and bolt force with respect to nut rotation for analytical and FE tightening cycles.

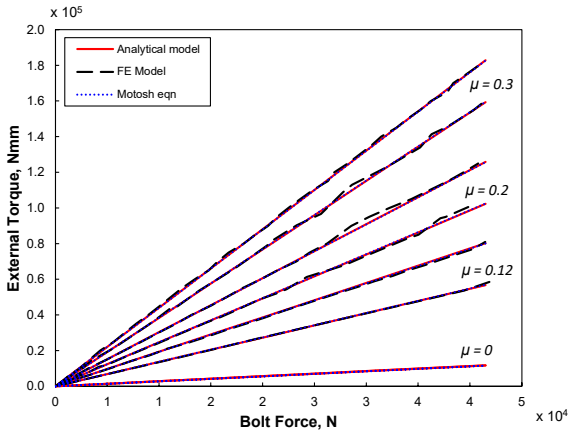

Figure 8. Torque and bolt force in M12 × 1.75 bolt for different friction coefficients.

As the analytical model shows good agreement with FE results and the Motosh model for the M12 bolt so far, a bigger-sized bolt such as the M36 × 4 hex bolt is also tested and compared between the analytical and Motosh models. Figure 9 shows that the current analytical model is diverse enough to encompass wide ranges of bolt sizes and coefficients of friction.

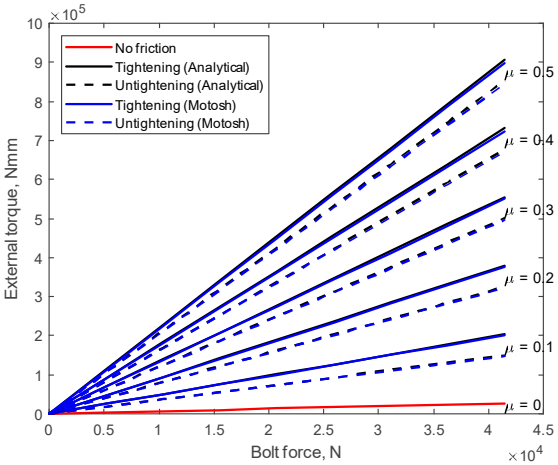

Figure 9. Comparison of analytical and Motosh models with torque and bolt force in M36 × 4 bolt for different friction coefficients.

Figure 10 presents the relationship between the coefficient of friction and the corresponding nut factor with different methods and bolt sizes. According to Bickford [3], the nut factor K is approximately 0.04 greater than the corresponding coefficient of friction. As can be seen in the figure, the curves of the analytical and Motosh models are superimposed to fit in a line and agree well with Bickford's assumption, the expression of which is as follows:

$$K = 1.16\mu + 0.02 \tag{23}$$

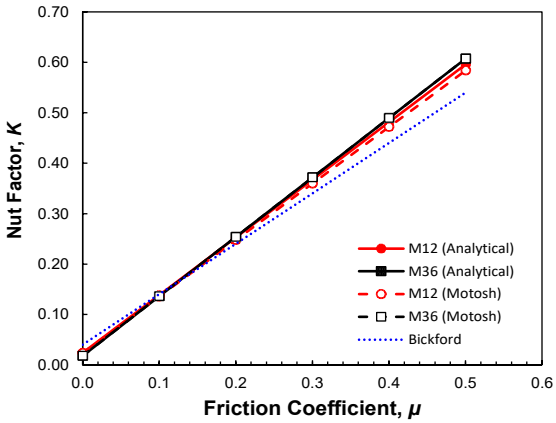

Figure 10. Comparison of nut factor as a function of friction coefficient.

To find the amounts of various torque components (T_b, T_t, and T_p) during both the tightening and subsequent untightening sequences resulting from the external torques (T_e), a detailed comparison of the analytical and FE model results for a particular coefficient of friction is presented in Figure 11. The results are quite satisfactory, as both agree very well. In particular, the amounts of torque components when the joint is at rest can be known when the input tightening torque is removed after achieving the desired bolt force. Table 2 shows the percentage difference of the different torque components between the analytical and FE models.

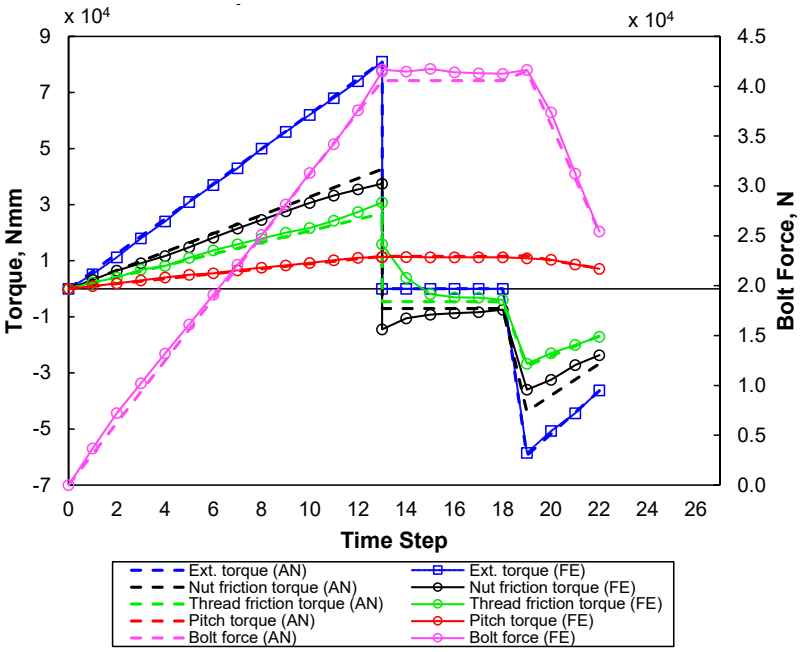

Figure 11. Analytical and FE results of torque components during tightening and untightening.

Table 2. Comparison of various torque components after tightening and untightening.

Torques	Tightening			Untightening		
	Analytical	FE	Percentage Difference (%)	Analytical	FE	Percentage Difference (%)
T_e	81,083	81,000	0.1	59,474	58,479	1.7
T_b	42,708	37,476	14	26,719	23,697	12.7
T_t	26,894	30,813	12.7	16,828	17,075	1.5
T_p	11,487	11,344	0.9	7188	7138	0.7

According to both the analytical and FE results, almost 85% of the input tightening torque is absorbed by the bearing and thread friction torque components in overcoming friction. The amount of the bearing friction torque is higher than that of the thread friction torque in both cycles, which was experimentally tested earlier by Grabon et al. [16]. Moreover, the amount of torque to untighten the joint after being tightened to the desired level is less than the required tightening torque according to both models, which can be seen in Figure 8.

5. Conclusions

The phenomenon of loosening of a bolted joint is complex in nature, especially when it comes to investigating critical parameters like individual torque components between the tightening and untightening sequences. This study introduces a comprehensive FE method to quantitatively assess the individual contribution and impact of the bearing friction, thread friction, and pitch torque components in a bolted joint. Also, it shows their fluctuations during the tightening and untightening sequences under static conditions. An analytical model is developed for the evaluation of the three torque components and compared with experimental data obtained from the literature [29], which was conducted on the M12 bolted joint during the tightening and untightening sequences. The validated analytical model is also tested against the FE modeling, and the results are compared well. A direct correlation between the angle of nut rotation to achieve the desired clamping force and the resultant input tightening torque shows logical agreement between them, which has a major role in the joint stiffness. Both models agree very well with the change in the coefficient of friction during the tightening and untightening of the bolted joint. Finally, the torque components are quantitatively measured and compared during tightening and untightening, including at the condition of rest. Given the versatility of the current approach, this study can serve as a valuable reference for future studies that examine the variations in torque components of joints subjected to repeated tightening and untightening over time, considering factors such as adhesion due to material corrosion and thread plastic deformations, relaxation, vibration, and self-loosening.

Author Contributions: R.I.R.: conceptualization, methodology, software, formal analysis, investigation, and writing—original draft preparation; A.-H.B.: project administration, methodology, resources, supervision, and writing—review and editing. All authors have read and agreed to the published version of the manuscript.

Funding: This research and the APC were funded by the Natural Sciences and Engineering Research Council of Canada (NSERC) through the Discovery Grant (RGPIN-202103780) and École de technologie supérieure.

Data Availability Statement: The data presented in this study are available on request from the corresponding author due to privacy.

Conflicts of Interest: The authors declare that they have no known competing financial interests or personal relationships that could have appeared to influence the work reported in this paper.

References

1. Li, L.; Yun, Q.-Q.; Tian, H.-F.; Cai, A.-J.; Cao, A.-Y. Investigation into the contact characteristics of rough surfaces with surface tension. *J. Braz. Soc. Mech. Sci. Eng.* **2019**, *41*, 343. [CrossRef]
2. Motosh, N. Development of design charts for bolts preloaded up to the plastic range. *ASME J. Eng. Ind.* **1976**, *98*, 849–851. [CrossRef]
3. Bickford, J.H. *An Introduction to the Design and Analysis of Bolted Joints*, 3rd ed.; Marcel Dekker: New York, NY, USA, 1997; pp. 154–196.
4. Juvinall, R.C.; Marshek, K.M. *Fundamentals of Machine Component Design*, 3rd ed.; Wiley: New York, NY, USA, 2000.
5. Kogut, L.; Etsion, I. A Static friction model for elastic-plastic contacting rough surfaces. *J. Tribol.* **2004**, *126*, 34–40. [CrossRef]
6. Nassar, S.A.; Yang, X. Torque-angle formulation of threaded fastener tightening. *J. Mech. Des.* **2008**, *130*, 024501. [CrossRef]
7. Nassar, S.A.; Zaki, A.M. Effect of coating thickness on the friction coefficients and torque-tension relationship in threaded fasteners. *J. Tribol.* **2009**, *131*, 021301. [CrossRef]
8. Nassar, S.A.; Barber, G.C.; Dajun, Z. Bearing friction torque in bolted joints. *Tribol. Trans.* **2005**, *48*, 69–75. [CrossRef]
9. Nassar, S.A.; Matin, P.H.; Barber, G.C. Thread friction torque in bolted joints. *J. Press. Vessel Technol.* **2005**, *127*, 387–393. [CrossRef]
10. Izumi, S.; Yokoyama, T.; Iwasaki, A.; Sakai, S. Three-dimensional finite element analysis of tightening and loosening mechanism of threaded fastener. *Eng. Fail. Anal.* **2005**, *12*, 604–615. [CrossRef]
11. Huang, J.; Guo, L.S. The research on the torque-tension relationship for bolted joints. *Key Eng. Mater.* **2011**, *486*, 242–245. [CrossRef]
12. Fukuoka, T. Finite element simulation of tightening process of bolted joint with a tensioner. *J. Press. Vessel Technol.* **1992**, *114*, 433–438. [CrossRef]
13. Jiang, Y.; Chang, J.; Lee, C.-H. An experimental study of the torque-tension relationship for bolted joints. *Int. J. Mater. Prod. Technol.* **2001**, *16*, 417–429. [CrossRef]
14. Liu, Z.; Zheng, M.; Yan, X.; Zhao, Y.; Cheng, Q.; Yang, C. Changing behavior of friction coefficient for high strength bolts during repeated tightening. *Tribol. Int.* **2020**, *151*, 106486. [CrossRef]
15. Zou, Q.; Sun, T.S.; Nassar, S.A.; Barber, G.C.; Gumul, A.K. Effect of lubrication on friction and torque-tension relationship in threaded fasteners. *Tribol. Trans.* **2007**, *50*, 127–136. [CrossRef]
16. Grabon, W.A.; Osetek, M.; Mathia, T.G. Friction of threaded fasteners. *Tribol. Int.* **2018**, *118*, 408–420. [CrossRef]
17. Fernando, A.; Lee, J.; Pokharel, T.; Gad, E. Improvements to torque versus tension relationship considering nut dilation effects. *Proc. Inst. Mech. Eng. Part C J. Mech. Eng. Sci.* **2022**, *236*, 3578–3594. [CrossRef]
18. Jiang, K.; Liu, Z.; Wang, Y.; Tian, Y.; Zhang, C.; Zhang, T. Effects of different friction coefficients on input torque distribution in the bolt tightening process based on the energy method. *J. Tribol.* **2022**, *144*, 071203. [CrossRef]
19. Zhang, J.; Feng, J.; Li, W.; Liao, R. Improving torque-tension relationship in bolted joints: Accurate threaded surface representation and pressure distribution considerations. *Mech. Based Des. Struct. Mach.* **2024**, 1–21. [CrossRef]
20. Fort, V.; Bouzid, A.-H.; Gratton, M. Analytical modeling of self-loosening of bolted joints subjected to transverse loading. *J. Press. Vessel Technol.* **2019**, *141*, 031205. [CrossRef]
21. Meyer, G.; Strelow, D. Simple diagrams aid in analyzing forces in bolted joints. *Assem. Eng.* **1972**, *15*, 28–33.
22. Sawa, T.; Maruyama, K. On the deformation of the bolt head and nut in a bolted joint. *Bull. JSME* **1976**, *19*, 203–211. [CrossRef]
23. Rousseau, R.I.; Bouzid, A.-H.; Zhao, Z. Accurate Evaluation of Bolt and Clamped Members Stiffnesses of Bolted Joints. In Proceedings of the ASME Pressure Vessels and Piping Conference, Virtual, 18 October 2021. [CrossRef]
24. Zhang, D.; Gao, S.; Xu, X. A new computational method for threaded connection stiffness. *Adv. Mech. Eng.* **2016**, *8*, 1–9. [CrossRef]
25. *BS 3643: Part 2*; ISO Metric Screw Threads. Limits and Tolerances for Fine Pitch Threads (Constant Pitch Series). BSI: Singapore, 1981. [CrossRef]
26. ANSYS Inc. *Ansys Workbench 19.1*; Version 2019; [Computer Program]; ANSYS Inc.: Canonsburg, PA, USA, 2019.
27. ASME. *Boiler and Pressure Vessel Code, Section II, Part A: Materials Specifications*, ASTM A193/A193M—Standard Specification for Alloy-Steel and Stainless Steel Bolting for High-Temperature or High-Pressure Service and Other Special Purpose Applications, Latest ed.; ASTM International: West Conshohocken, PA, USA, 2024.
28. ASME. *Boiler and Pressure Vessel Code, Section II, Part A: Materials Specifications*, ASTM A285/A285M—Standard Specification for Pressure Vessel Plates, Carbon Steel, Low- and Intermediate-Tensile Strength, Latest ed.; ASTM International: West Conshohocken, PA, USA, 2017.
29. Eccles, W. A New Approach to the Checking of the Tightness of Bolted Connections. In Proceedings of the Lubrication, Maintenance and Tribotechnology (LUBMAT), Manchester, UK, 25–27 June 2014.